~~Sent 8/23~~
~~Revised~~
In press

# ADSORPTION AND TRANSPORT OF U(VI) IN SUBSURFACE MEDIA

M. 0. Barnett*, P. M. Jardine, S. C. Brooks, and H. M. Selim

M. 0. Barnett, P. M. Jardine, S. C. Brooks, Environmental Sciences Division, Oak Ridge National Laboratory, P.O. Box 2008, Oak Ridge, Tennessee 37831-6038. H. M. Selim, Department of Agronomy, 104 Sturgis Hall, Louisiana State University, Baton Rouge, LA 70803. This research was sponsored by the U.S. Department of Energy, Office of Biological and Environmental Research, Environmental Management Science Program, under the direction of Dr. Paul Bayer. Oak Ridge National Laboratory is managed by Lockheed Martin Energy Research Corporation under contract DE-AC05-96OR22464 with the U.S. Department of Energy. This research was supported in part by an appointment to the Oak Ridge National Laboratory Postdoctoral Research Associates Program administered jointly by the Oak Ridge Institute for Science and Education and Oak Ridge National Laboratory. *Corresponding author (barnettm@eng.auburn.edu), current address Department of Civil Engineering, 208 Harbert Engineering Center, Auburn University, AL, 36849-5337.

# ADSORPTION AND TRANSPORT OF U(VI) IN SUBSURFACE MEDIA

## ABSTRACT

U(VI) adsorption and transport in three natural, heterogeneous subsurface media were investigated in batch and column experiments. The rate of U(VI) adsorption to the natural samples was rapid over the first few hours of the experiments, and then slowed appreciably after twenty-four to forty-eight hours. The adsorption of U(VI) to the samples was also nonlinear, suggesting a decreasing attraction for the surface with increased surface loading. The extent of adsorption on each of the media was strongly pH-dependent, increasing sharply as the pH increased from 4.5 to 5.5 and then decreasing sharply over the pH range 7.5 to 8.5 as the concentration of dissolved carbonate and U(VI)-carbonate complexes increased. The similarities in the pH-dependent behavior between the three materials despite differences in bulk mineralogy was likely+ due to the similar Fe contents of the materials. The transport of U(VI) through packed columns of the soils and sediments was significantly retarded but reversible. The local equilibrium assumption and the batch-measured adsorption isotherms dramatically underestimated the degree of retardation observed in the columns. The U(VI) displacement experiments were modeled with the one-dimensional advective-dispersive equation and several different model formulations describing the interactions of U(VI) with the solid phase. These models were able to fit the observed breakthrough curves within 0.1 root mean square error of the initial concentration.

Uranium is introduced into the environment from the processing of uranium ores into nuclear fuels and materials. Uranium mining, milling, processing, enriching, and disposal all have the potential to contaminate groundwaters. In addition, natural and anthropogenically-accelerated (e.g., through irrigation (Duff and Amrhein, 1996)) U mobilization also occurs in areas with high natural background U concentrations. Uranium is a long-lived radionuclide with a suite of radioactive daughter products which can pose a human health and ecological risk. U(VI) is the thermodynamically stable form of U in oxic groundwaters and interacts strongly with solid phases. U(VI)-particle interactions govern the 'transport of U(VI) and ultimately the fate and distribution of uranium in the subsurface.

Iron-containing minerals in particular strongly adsorb U(VI) (Casas et al., 1994; Ticknor, 1994) and the interactions of U(VI) with pure Fe-mineral phases such as ferrihydrite (Waite et al., 1994), goethite (Kohler et al., 1992; Tripathi, 1983), amorphous iron hydroxide (Morrison et al., 1995), and hematite (Hsi and Langmuir, 1985) have been thoroughly investigated. In most cases, these studies have focused on the pH-dependent adsorption of U(VI) in batch experiments and have used different surface complexation model (SCM) formulations to describe the data. The adsorption of U(VI) to clay minerals is more complex, due to the larger variety of potential sorption sites. McKinley et al. (1995) and Turner et al. (1996) investigated the adsorption of U(VI) to clay minerals. They used a multiple site model where U(VI) could adsorb on both fixed charge and variable charge sites, with the variable charge edge sites modeled as gibbsite and silica analogs. The adsorption of U(VI) to other pure mineral phases such as sulfides (Wersin et al., 1994) and carbonates (Morse et al., 1984) have also been investigated.

Fewer studies have focused quantitatively on the adsorption of U(VI) to heterogeneous subsurface materials and its effects on U(VI) transport under dynamic (flowing) conditions. Voudrias and Means (1993) studied the adsorption and transport of U(VI) to halites, carbonates, and mudstones of the Palo Duro Basin in Texas. Predicted effluent curves based on the local equilibrium assumption and a linearized, batch-measured retardation coefficient underestimated the degree of retardation observed in column experiments. Sims et al. (1996) studied the transport of U(VI) through intact natural sandstone columns. Coupled chemical equilibrium-transport models were used to predict the extent of U(VI) migration within the cores based on SCM constants from U(VI) adsorption to silica and, the local equilibrium assumption. However, U(VI) transport in the columns was generally less than predicted by the model. Kohler, et al. (1996) investigated the adsorption of U(VI) to quartz particles in batch and column experiments as a function of U(VI) concentration, ligand concentration, and pH. A non-electrostatic SCM was used to model both batch adsorption and reactive solute transport in the column. The independently-measured batch parameters did not accurately predict the column breakthrough data, both over- and under-predicting the retardation in different experiments. Various formulations of the SCM were fit to the column data. These independently fitted parameters were able to qualitatively predict the breakthrough curves from columns with an added ligand (fluoride).

The purpose of this paper is to describe the results of an investigation into the adsorption and transport of U(VI) in natural, heterogeneous subsurface media. Our goal was to provide an improved understanding and predictive capability of U(VI) transport at contaminated Department of Energy (DOE)

sites in an effort to better characterize the risk of contaminant migration and evaluate potential cleanup scenarios. Adsorption and transport experiments were conducted on three subsurface materials acquired from the Oak Ridge Reservation in East Tennessee, the Savannah River Site on the Georgia-South Carolina border, and the Hanford Reservation in Southeastern Washington. All three DOE sites have a history of U waste disposal and subsurface contamination. Specific objectives of the investigation were: 1) to measure the adsorption of U(VI) on subsurface materials from these locations possessing different physical, chemical, and mineralogical properties, 2) to measure the effect of U(VI) concentration and pH on the extent of adsorption and 3) to measure and model U(VI) transport in packed columns of the these media.

# MATERIALS AND METHODS

## Soil and Sediment Description

Bulk samples of subsurface material were acquired from three geographically distinct locations within the United States: the Oak Ridge (OR) Reservation in East Tennessee, the Savannah River (SR) site on the Georgia-South Carolina border, and the Hanford (HF) Reservation in Southeastern Washington. Soils from OR were acquired at the 1.5 m depth within the C-horizon of a weakly-developed Inceptisol that has weathered from interbedded shale-limestone sequences. The limestone has weathered to massive clay lenses devoid of carbonates and the more-resistant shale has weathered to a highly fractured saprolite. Solid-phase minerals are heavily coated with Fe-oxides and to a lesser extent Mn-oxides. The soils are nearly identical to those used in the disposal of low-level and transuranic wastes on

the OR reservation. Sediments from the SR site were acquired from the 45 m depth of the McBean formation on the Atlantic coastal plain near the Old Burial Ground site. The media is dominated by sand-size quartz that is coated with Fe-oxides. One-fourth of the sediment mass is composed of occluded clays that are resistant to weathering due to Fe-oxide coatings. HF subsurface materials were acquired from the Upper Ringold Formation near the Hanford site. The sediments were sampled on the White Bluffs -60 m above the Columbia River from a freshly-exposed escarpment of -1 m (Zachara et al., 1995). The material is predominately sand-sized quartz with discrete Mn- and Fe-oxide minerals. Select physical, chemical, and mineralogical properties of the three media are presented in Table 1. Each of the bulk samples was air-dried and sieved through a 2 mm screen prior to use.

## Batch Experiments

Batch adsorption experiments were conducted in polycarbonate centrifuge tubes at room temperature (295.5 ±0.5 K) and a constant ionic strength (0.01 or 0.1 M). For adsorption isotherm measurements, thirty milliliters of air-saturated 0.01 N $NaNO_3$, pH-adjusted to the pH of the solid phase, were added to 0.1 g of solid phase. For pH-adsorption edge measurements, thirty milliliters of 0.1 N $NaNO_3$ was added to 0.1 g of solid phase' and the solutions were repeatedly pH adjusted with 0.1 N NaOH or $HNO_3$ and then bubbled with air using an aquarium pump (to ensure the samples had reached equilibrium with atmospheric carbon dioxide) until a constant pH was reached. Using this method, the average sample pH drift over the course of the experiment was <0.1 units for most experiments. Sample pH was measured with a pH meter and combination electrode using $NaNO_3$ as the outer fill solution to prevent chloride contamination of the samples which

The velocity, bulk density, and volumetric water content were measured or calculated from direct physical measurements. The solute dispersion coefficient was estimated independently by fitting an analytical solution of Equation 2 to the bromide breakthrough curve using D as the adjustable parameter with CXTFIT (Parker and van Genuchten, 1984).

Observed U(VI) displacement experiments were modeled with the Multireaction Transport Model (Ma and Selim, 1997; Selim et al., 1990). Several different formulations were used to model the interactions between U(VI) and the solid phase based on 1) local adsorption equilibrium, 2) rate-limited adsorption or 3) a combination of the two. Assuming local equilibrium-governed adsorption and using the Freundlich isotherm and constants measured in the batch experiments, the governing adsorption equation is

$$\frac{\partial q_e}{\partial t} = K_f n C^{n-1} \frac{\partial C}{\partial t} \tag{3}$$

where $q_e$ is the concentration (M/M) of U(VI) adsorbed on equilibrium sites. As some of the observed data indicated the presence of rate-limited adsorption, an adsorption rate equation was considered of the form

$$\frac{\partial q_k}{\partial t} \quad \frac{\theta}{\rho} k_1 C^m \quad k_2 q_k \tag{4}$$

where $q_k$ is the adsorbed concentration (M/M) of U(VI) on kinetic sites, $k_1$ and $k_2$ are the adsorption-desorption rate constants (t-l), and m is the order of the reaction.

pH. Column hydrodynamics were measured subsequent to the experiments by introducing a step input of a bromide-containing solution to the columns and measuring the concentration of bromide in the effluent by ion chromatography. The properties of the columns were similar with a porosity of 0.45, a dispersion coefficient of 3.2 $cm^2/hr$ (column Peclet number 5.2), and a bulk density of 1.5 $g/cm^3$. The fluid residence time in the columns was 0.18 hr.

## Modeling

The Freundlich equation

$$q = K_f C^n \tag{1}$$

was used to describe the adsorption isotherms where q and C are the concentration of U(VI) on the solid (mg/kg) and in the aqueous (mg/L) phases, respectively, $K_f$ is the adsorption capacity parameter, and n is the adsorption intensity parameter. Values of $K_f$ and n were determined by fitting Equation 1 to the data for each media using non-linear least squares regression analysis assuming constant absolute error.

The column experiments were modeled using the one-dimensional advective-dispersive equation

$$\frac{\partial C}{\partial t} = D\frac{\partial^2 C}{\partial x^2} - v\frac{\partial C}{\partial x} - \frac{\rho}{\theta}\frac{\partial q}{\partial t} \tag{2}$$

where D is the solute dispersion coefficient ($L^2/t$), v is the mean pore-water velocity (L/t), x is the distance along the column (L), $\rho$ is the column bulk density ($M/L^3$), $\theta$ is the volumetric water content ($L^3/L^3$), and t is the time.

could have interfered with U(VI) measurements. The samples were spiked with a small volume of U(VI) stock solution to achieve the desired concentration and enough NaOH to neutralize the acid from the added stock solution. MINTEQA2 (Allison et al., 1991) was used to determine the upper concentration limit of U(VI) to minimize supersaturation with respect to U minerals. The samples were then placed on a reciprocating shaker table and gently agitated for designated time periods. After the desired reaction time, the samples were removed from the shaker table, centrifuged and/or filtered to remove particles >0.45 μm and separate aliquots of the supernatant were analyzed for pH and U(VI) with a kinetic phosphorescence analyzer. The adsorbed U(VI) concentration was calculated from the difference between the initial and final U(VI) concentration. Blank samples were included with no soil to verify the added U(VI) concentration and with no added U(VI) to verify no U(VI) was desorbing from the original material. For the OR material, separate samples were also analyzed for Ca, Mg, Si, Al, Fe, and Mn using inductively-coupled plasma atomic emission spectroscopy.

## Transport Experiments

Transport experiments were conducted in 1-cm diameter glass columns at room temperature (295.5 L-O.5 K) and a constant ionic strength (0.01 M). Two grams of each media was dry-packed to a depth of 1.7 cm. The columns were slowly flushed from the bottom using 0.01 N $NaNO_3$, pH-adjusted to the soil pH, until air spaces were no longer visible. A step input of U(VI) in a 0.01 N $NaNO_3$ background matrix was introduced to each of the columns at a specific discharge of 4.3 cm/hr. After the desired breakthrough period, the inlet solution was switched back to a U(VI)-free, 0.01 N $NaNO_3$ solution. Effluent samples were collected with a fraction collector and analyzed for U(VI) and

Various combinations of Equations 3 and 4 representing different model formulations were used to describe the interactions between aqueous U(VI) and the solid phase. The models used were: a non-linear equilibrium model (NLE, equation, 3), a coupled non-linear equilibrium, first-order kinetic model (NLE-FOK, equations 3 and 4 with m fixed at one), a first-order kinetic model (FOK, equation 4 with m fixed at one), and a fractional order kinetic model (FRK, equation 4 with m as an adjustable parameter). For the NLE-FOK model, the total adsorbed U(VI) concentration was'the sum of the adsorbed concentrations on both equilibrium and kinetic sites.

Each model formulation differed only in the equations used to describe the interaction of U(VI) with the solid phase. Equation 2 and the governing solute-sorbent equations were solved numerically using finite difference approximations of the governing partial differential equations subject to a third-type boundary condition at the column entrance and a Newman boundary condition at the column exit (Selim et al., 1990). The models were fit to the data with non-linear least squares curve fitting. The agreement between the model-calculated and experimentally-measured values was quantified by the root mean square error (RMSE)

$$\mathrm{RMSE} = \left[ \frac{1}{n_d - n_p} \sum_{i=1}^{n_d} \left( \frac{C_i(t) - \hat{C}_i(t)}{C_0} \right)^2 \right]^{\frac{1}{2}} \tag{5}$$

where $n_d$ is the number of data points, $n_p$ is the number of adjustable parameters, i is an index, $C_i(t)$ and $\hat{C}_i(t)$ are the measured and calculated values of the concentration at time t, and $C_0$ is the inlet concentration. The RMSE is an estimate of the standard deviation between measured and

calculated concentrations expressed in dimensionless form as a fraction of the inlet concentration, where lower values of RMSE indicate a better fit of the model to the data. Models containing different numbers of adjustable parameters were compared to determine which provided the statistically better fit using the extra sum of squares principle (Kinniburgh, 1986).

# RESULTS AND DISCUSSION

## Batch Kinetic Experiments

In order to examine U(VI) adsorption dynamics and determine the time frame when adsorption equilibrium was approached, batch kinetic experiments were conducted for the media at constant pH and ionic strength. The results are shown plotted as a fraction of the initial concentration remaining in solution versus time (Figure 1). The initial U(VI) concentration of the HF sediment was lower than the other two materials to minimize the supersaturation of $\beta$-$UO_2(OH)_2(s)$ at the higher indigenous pH of this material. In these experiments, the soil solution pH was adjusted to the natural, unaltered pH of the solid phase (Table 1).

The OR and HF materials exhibited a classic biphasic loss of U(VI) from solution which is characterized by an initial rapid decrease in aqueous concentration over the first eight to twenty-four hours followed by a slower rate of decrease over the remainder of the experiment (Figure 1). In contrast, the SR sediment exhibited an initially rapid (<1 hr) loss of U(VI) from solution followed by a slight increase in aqueous concentration over the remainder of the experiment (145 hr). This observation cannot be attributed to experimental error based on the precision of replicate samples analyzed at the same time (Figure 1). Similarly, when plotted on the adsorption isotherm

(discussed below), the initial points fell slightly above the isotherm (i.e., at a given aqueous concentration, more adsorption was observed initially than after a longer period of equilibration). Bruno et al. (1995) observed this same phenomenon in the presence of precipitating Fe-oxyhydroxides and attributed it to a rapid adsorption of U(VI) to the Fe surface followed by a slower structural rearrangement on the solid surface. Since Fe-containing solids are important adsorption-controlling phases in these media, the adsorption rate behavior in the SR sediment may likewise reflect a rapid adsorption of U(VI) to the Fe surface followed by a slower rearrangement to a more structurally or energetically favored arrangement. For all three media, after twenty-four to forty-eight hours, the aqueous concentration changed by less than 5% over the next -100 hours of the experiment. Although further long-term uptake of U(VI) can not be ruled out, for the purposes of batch experiments, adsorption equilibrium was assumed to be reached after forty-eight hours.

## Batch Adsorption Equilibrium Experiments

After establishing the time required to approach adsorption equilibrium, batch experiments were conducted for each subsurface material at the natural, unaltered pH of the solid phase (Table 1) and over a range of initial aqueous concentrations. The aqueous concentration range was again lower for the HF sediment to minimize the potential for precipitation of $\beta$-$UO_2(OH)_2$ at the higher pH of this sediment. For all three materials, the adsorption isotherm was non-linear (Figure 2). Non-linear adsorption is characteristic of a decreasing sorbent-sorbate affinity with an increasing extent of adsorption (Sposito, 1984) and may reflect U(VI) adsorption to different types of sites as a function of surface loading. Morris et al. (1994) and Chisholm-Brause et al. (1994) detected spectroscopically distinct adsorbed U(VI) species on the surface

of pure clay minerals which they attributed to U(VI) adsorption on sites with distinct structures or energy. In heterogeneous media, like those used in this study, there is the potential for an even larger variety of surface sites. Of the conventional non-electrostatic isotherms, the data was best described by the Freundlich isotherm (Equation 1, Table 2).

## pH Adsorption Edges

The extent of adsorption at a given aqueous concentration increased with the pH of the three samples (Figure 2), with the alkaline HF sediment showing the largest sorption capacity followed by the acidic OR soil and the SR sediment. To examine the importance of pH on adsorption to a given material, batch adsorption experiments were conducted for each material at a constant initial U(VI) concentration (1 mg/L) over a pH range of 2.5 to 10 (Figure 3). The experiments were conducted at a higher ionic strength (0.1 versus 0.01 M) than other experiments reported here to minimize changes in ionic strength due to the increasing absorption of carbon dioxide at higher pH. Additional experiments (results not shown) indicated that changing the ionic strength from 0.01 to 0.1 M also influenced adsorption. The percentage of U(VI) adsorbed, at a given pH and total U(VI) concentration, decreased as the as the ionic strength increased from 0.01 to 0.1 M, suggesting competition for sorption sites by the $Na^+$ counter ion in the background electrolyte. These results indicate that U(VI) adsorption on the solid phase may be due to outer-sphere surface complexation and may explain why U(VI) adsorption in displacement experiments was nearly 100% reversible in a Na+ matrix as discussed below. Despite the influence of ionic strength on adsorption, the results (Figure 3) illustrate the effects of pH at a constant ionic strength of 0.1

M. At an ionic strength of 0.1 M, the adsorption of U(VI) to fixed charge sites is minimal, as little if any adsorption is observed at low pH.

Aqueous-phase pH was a controlling factor in U(VI) adsorption (Figure 3). As is the case for most cationic metals, U(VI) exhibited a classic pH adsorption edge; the fraction of U(VI) adsorbed 'on each soil or sediment increased sharply with pH over the relatively narrow pH range of -4.5 - 5.5. Unlike most other cationic metals, however, the degree of adsorption decreased sharply again as pH increased over another relatively narrow pH range of -7.5 - 8.5. This second or "reverse" pH adsorption edge has been observed for U(VI) on pure Fe mineral phases such as goethite, hematite, ferrihydrite and amorphous iron hydroxide (Hsi and Langmuir, 1985; Tripathi, 1983; Waite et al., 1994) in open systems. This behavior has been explained as a consequence of 1) the increase in the dissolved carbonate concentration with pH at constant carbon dioxide partial pressure and 2) a concurrent increase in the concentration of U(VI)-carbonate complexes.

The calculated system speciation and the total dissolved carbonate concentration change as a function of pH in the experimental system (Figure 4). As pH increases in an open system, the concentration of dissolved carbonate increases and the degree of U(VI) complexation with carbonate increases as well. Since the U-carbonate species are neutral or anionic, electrostatic interactions with the solid phase will be negligible. In addition, competition with U(VI) for surface sites from dissolved carbonate and bicarbonate anions will also increase as the pH and total carbonate concentration increase. These phenomena are likely responsible for the reversal in the U(VI)-pH edge in open systems.

subsurface media and its effect on aqueous-phase U(VI) transport, column transport experiments were conducted for each of the soils and sediments.

The transport of U through the three columns (Fig. 5 - 7) was significantly retarded relative to the transport of the conservative tracer bromide (not shown). Complete U(VI) breakthrough did not occur until after 3000 pore volumes for the column exhibiting the fastest breakthrough (SR) and had not occurred even after 6000 pore volumes for the column exhibiting the slowest breakthrough (HF). Qualitatively, the relative degree of retardation exhibited in each column agreed with the relative degree of adsorption observed in the batch-measured isotherms (Figure 2) and the pH adsorption envelopes (Figure 3). The breakthrough of U(VI) in the SR column (pH 4.1) occurred before the breakthrough from the OR column (pH 4.7) which occurred significantly before the breakthrough from the HF column (pH 6.8).

The shape of the breakthrough curves was slightly different for the three columns, although each breakthrough curve was asymmetric. Asymmetric breakthrough curves are indicative of 1) nonlinear adsorption and/or 2) rate-limited adsorption (Jardine, 1991), both of which were observed in kinetic and equilibrium batch experiments (Figure 1 - 2). For all three media, the batch-measured adsorption isotherms were markedly nonlinear (Figure 2). In addition, there was a significant potential for time-dependent adsorption given the short residence time in the column (0.18 hr) relative to the time required to reach adsorption equilibrium (24-48 hr).

The overall column U(VI) mass balance was checked by calculating the mass of U(VI) adsorbed during the adsorption phase and desorbed during the desorption phase by numerical integration of the experimental breakthrough

Although the adsorption edges shown for the three soils or sediments are not identical, there are many similarities. All three media exhibited similar $pH_{50}$-1 and -2 (the pH where 50% of the U(VI) was adsorbed at lower and higher pH respectively), $pH_{max}$ (the pH where maximum adsorption occurs), and maximum degree of adsorption (Table 3). The relative similarities between these values despite differences in bulk mineralogy suggest the adsorption-controlling phase in each soil or sediment may be similar. Fe-oxyhydroxides are known to strongly interact with U(VI). The bulk Fe content of all three materials is very similar, ranging from 25.3 to 25.8 g/kg (Table 1). Fe-oxyhydroxides coat the clays in OR and SR materials and exist as discrete phases and coatings on silica in the HF sediment. They are also the dominant pH-dependent charged surface in these soils. The similar pH-dependent U(VI) adsorption edges and total Fe content for these materials suggest the dominance of the Fe-oxyhydroxides in controlling U(VI) adsorption. X-ray absorption spectroscopy (XAS) data are being analyzed to test this hypothesis (S.E. Fendorf et al., Stanford University, unpublished results, 1998).

## Transport Experiments

Although batch experiments can provide useful mechanistic information about solute-sorbent interactions, they have limited applicability to actual subsurface transport due to 1) the low solid-solution ratio compared to porous media 2) the potential buildup of reaction products and intermediates in the closed system 3) the lack of hydrodynamic mass-transport limitations which may occur in porous media and 4) particle abrasion resulting in potential alterations in mineral reactivity. To better investigate adsorption of U(VI) to

curves. Quantitative U(VI) recovery was obtained in all columns indicating the U(VI) adsorption was readily reversible for these materials. Over 98% of the U(VI) sorbed to the SR sediment and over 95% of the U(VI) sorbed to the OR soil during the adsorption phase was recovered during the desorption phase. Over 90% of the U(VI) mass adsorbed to the HF sediment in the adsorption phase was also recovered in the desorption phase. Given the relatively small amounts of U(VI) involved (maximum amount of U(VI) absorbed in any column < 5 mg), close to complete mass recoveries within experimental errors were obtained.

## Modeling Results

To provide an improved understanding of U(VI) transport, quantitative transport modeling was performed on the U(VI) effluent data using a multireaction transport model.. Initially it was of interest to determine how well the batch-measured adsorption isotherms predicted transport through the columns. Simulated breakthrough curves based on the batch-measured adsorption isotherms and the local adsorption equilibrium assumption (the NLE model) did not adequately predict the breakthrough of U(VI) from any of the columns, with RMSE ranging from 0.250 to 0.568 (Fig. 5-7, Table 4).

One potential reason for the discrepancy noted between the NLE-predicted and observed breakthrough curves is non-equilibrium (i.e., rate-limited) adsorption-desorption, which could be manifested due to the differences in hydraulic residence time between the batch (48 hours) and column (0.18 hour) experiments. Evidence of rate-limited adsorption can be seen in the observed breakthrough curve for the SR sediment compared to the NLE-predicted breakthrough curve (Figure 5). The observed

breakthrough occurred initially earlier than predicted by the equilibrium model. Similarly, the observed effluent concentration decreased more rapidly than predicted during the desorption phase. Both these phenomenon are indicative of rate-limited adsorption-desorption.

An additional reason for the discrepancy between the NLE-predicted and observed breakthrough curves is the larger adsorption capacity the materials exhibited in the column experiments compared to the batch experiments. This observation can be noted by comparing the area above both the observed and NLE-predicted effluent curves during the adsorption phase; this area is proportional to the amount of U(VI) adsorbed at any point in time. By integrating the areas above the NLE-predicted and observed breakthrough curves during the adsorption phase, it was determined that 2.0, 2.2, and 1.7 times as much U(VI) was ultimately adsorbed in the SR, OR, and HF columns respectively than was predicted on the basis of the batch-measured adsorption isotherms. . The reason for this discrepancy is unclear, but in *general, parameters measured in batch experiments often do not translate well into column transport experiments (Zachara and Streile, 1991). The data of Kohler et al. (1996) and Voudrias and Means (1993) provide specific evidence of discrepancies between U(VI) adsorption/transport in batch and column experiments.

There are several fundamental differences between the adsorption environments in batch and column experiments which could produce such differences. The mean' U(VI)-solid phase contact time in column experiments was significantly longer than in batch experiments, which lasted for 48 hours, while U(VI) inputs to the columns lasted for at least 23 days. The longer U(VI) contact time with the solid phase may have allowed for migration of

adsorbed U(VI) into micropores of the solid phase (e.g., interlayer sites of 2:1 clays), freeing up additional surface sites, and/or structural rearrangement of the adsorbed U(VI) phase allowing more adsorption. In addition, in batch experiments, all the U(VI) was added in one spike at the beginning of the experiment, while in the column experiments the solid. phase (except immediately at the column entrance) experiences a gradual increase in U(VI) concentration. This gradual increase in concentration could lead to a different and more efficient arrangement of U(VI) on the surface. Finally, in batch experiments, solutes dissolving from the solid phase which would be rapidly flushed out in columns can build up in solution, inhibiting U(VI) adsorption.

In order to test whether or not these differences could explain the discrepancies in observed adsorption capacity between batch and column experiments, three additional batch adsorption isotherms for the OR material were measured (Figure 2b). An additional adsorption isotherm (isotherm 2) was measured under the same conditions as the original isotherm (isotherm 1) but with a one month equilibration time to test the importance of additional U(VI)-solid phase contact time. A third isotherm (isotherm 3) was measured under the same conditions as isotherm 1, except that the U(VI) was added in three equal increments over approximately 48 hours to determine if a more gradual buildup in U(VI) influenced adsorption. Finally, a fourth isotherm (isotherm 4) was measured in the presence of small amounts of added Si (18 μM), Ca (50 μM), and Mg (48 μM), which is approximately the same amount of Si, Ca, and Mg dissolved from the solid phase over the course of the original forty-eight hour batch experiment.

duration batch experiments. Although the solutions used in the column experiments were theoretically undersaturated with respect to $UO_2(OH)(s)$, recent research has shown that surface precipitation of metal hydroxides can occur on solid oxyhydroxides even when the systems are undersaturated with respect to the pure metal hydroxide (Towle et al., 1997). However, the interactions of U(VI) with the'solid phase were completely reversible. The reductive precipitation of $UO_2(s)$ is not likely to have occurred, as the solutions used in the column experiments were air-saturated, and the presence of oxygen would inhibit the reduction of U(VI). In the absence of direct spectroscopic evidence, it is not possible to identify the specific mechanism(s) by which U(VI) was retained in the columns. However, in a column packed with pure quartz sand, complete breakthrough of U(VI) was achieved in less than 100 pore volumes (results not shown), indicating any retention observed in the columns was due to the interaction of U(VI) with each of the specific media.

In order to better quantitatively model the results, several different model formulations were investigated for their ability to describe the data. The underlying formulations of these models, which are different in each case, are not meant to represent specific sorption mechanisms. A model incorporating the batch-measured adsorption isotherm and a reversible first-order adsorption-desorption rate expression was used. This model (the NLE-FOK model) is a two-site model, with adsorption equilibrium being maintained on equilibrium sites and rate-limited adsorption-desorption occurring on kinetic sites. The total adsorbed concentration is the sum of the adsorbed concentration on both the kinetic and equilibrium sites.

The results (Figure 2b) suggest these additional factors may influence adsorption, at least to a limited extent. The data from isotherms 1 and 3 were quite close, with very little difference between fitted isotherms. However, there was evidence that longer equilibrium times and the presence of ions dissolved from the solid phase could influence adsorption. As hypothesized, a one month equilibration time did result in more adsorption capacity. Similarly, the addition of Ca, Mg, and Si resulted in lower adsorption capacity. Although the concentrations of added Si, Mg, and Ca are quite low, they are on the same order as the maximum amount of U(VI) added to the soil (40 μM). These added solutes could then potentially compete with U(VI) for non-specific adsorption sites (e.g., CEC sites). When constants for each of the isotherms were used in the NLE 'model, the predicted breakthrough curve shifted slightly (Figure 6). It is not possible 'to determine the absolute magnitude of these effects, since some buildup of dissolution products in batch experiments is inevitable. However, these observations indicate that at least some of the difference between the adsorption capacity observed in batch and column experiments can be explained by differences in the adsorption environments in batch and column experiments, and there are, undoubtedly, other differences as well. Szecsody et al. (1998), for example, have suggested that particle-scale heterogeneity may be responsible for differences in observed batch and column adsorption characteristics for heterogeneous media. Whatever the cause, these results illustrate a fundamental difference between U(VI) adsorption in batch and column experiments.

The additional sorption capacity observed in the column could also be the result of the slow precipitation of $UO_2(OH)(s)$ and/or the reductive-precipitation of $UO_2(s)$ which was not observed in the relatively short

For the equilibrium sites, the batch-measured adsorption isotherm constants (Table 2) were used, while the kinetic parameters were determined by fitting the model to the column breakthrough data. The batch kinetic experiments were not used to provide independent estimates of the adsorption/desorption rate constants since the' experimental conditions were dramatically different. The original purpose of the batch kinetic experiments was to determine the time frame required to approach adsorption equilibrium. Thus the data points were largely outside the data range appropriate for the column study (i.e., the first batch data points were taken at 0.25 hours but the total column residence time was only 0.18 hour). However, the batch kinetic data were extrapolated back to shorter times to provide initial estimates of the kinetic parameters for the model.

Adding a kinetic component to the equilibrium model effectively allows for more total adsorption than predicted on the basis of the equilibrium model alone (e.g., the total U(VI) adsorbed at any time is equal to the U(VI) adsorbed on equilibrium sites plus the U(VI) adsorbed on kinetic sites). Inclusion of this additional adsorption capacity greatly improved the model's ability to match the observed U(VI) breakthrough (Fig. 5-7), with the resulting RMSE ranging from 0.047 - 0.094 (Table 4). Although the NLE was a purely predictive model (i.e., not fitted to the data) and the NLE-FOK model had two adjustable parameters, the improvement in the model fit was still significant ($p<0.05$) even when considering the additional adjustable parameters. The relative error estimates for the adjustable parameters in the NLE-FOK model were large in some cases which reflects the auto-correlation between the fitted parameters (Kinniburgh, 1986).

Although the NLE-FOK model was able to describe the data within 0.1 RMSE, two additional model formulations, a first-order kinetic (FOK) model and a fractional order kinetic model (FRK), were tested to determine whether improved model fits could be obtained. The FOK model is a purely kinetic (i.e.; no equilibrium sites) first order adsorption/desorption rate model. The FRK model is identical except that the reaction order (m) is used as an additional fitted parameter rather than assuming the adsorption rate is first order with respect to the aqueous U(VI) concentration.

The FOK model was no more successful than the NLE-FOK model in fitting the breakthrough data, with the resulting RMSE ranging from 0.053 - 0.079 (Table 4, calculated curves not shown for clarity). There was, however, an improvement in the relative error estimates of the parameters due to a decrease in the auto-correlation between the fitted parameters. The FRK model was able to fit the data better than any of the models tested, with RMSE ranging from 0.036 to 0.042 (Fig. 5-7, Table 4). Despite the inclusion of an additional fitted parameter (m) in the FRK model, the model was able to fit the data significantly ($p<0.05$) better than the NLE-FOK model. The relative errors in the parameter estimates were also decreased due to a decrease in the auto-correlation between the fitted rate constants.

It is not possible to establish that one model is more mechanistically correct simply on the basis of curve fitting, although the consistently better fit of the fractional order kinetic model compared to the first-order kinetic models may be indicative of the processes controlling the adsorption rate. Phenomenologically, a non-linear rate dependence ($m<1$) indicates that the reaction rate per unit concentration is higher at low concentrations. Conceptually, such a dependence could be due to a variety of causes. The

suggest. that the iron content, which was similar for each media, strongly controlled pH-dependent adsorption.

In transport experiments, U(VI) was significantly retarded due to adsorptive interactions with the porous media, requiring thousands of pore volumes to achieve breakthrough. The observed breakthrough curves were highly asymmetric, indicating the existence of nonlinear and/or rate-limited adsorption. A one-dimensional transport model based on local adsorption equilibrium and adsorption isotherms measured in independent batch experiments underestimated the ultimate degree of adsorption observed in packed columns. Adding a rate-dependent adsorption reaction to the model significantly improved the ability of the model to describe the data. Several rate-dependent adsorption model formulations were able to fit the observed breakthrough curves within an RMSE of <0.1. The data for all three column experiments was best fit with a fractional order kinetic model, suggesting that the adsorption rate dependence may be nonlinear as well. Knowledge of these aspects of U(VI) adsorption and transport in natural, heterogeneous subsurface media will be useful in the development of models to predict U(VI) migration and test remediation scenarios at contaminated sites.

first-order kinetic models used in this investigation implicitly conceptualize an infinite number of surface sites. Thus the adsorption (forward) reaction rate is modeled as dependent only on the aqueous concentration. An actual rate dependence on the concentration of a finite number of vacant sites could result in an apparent non-linear dependence on the aqueous concentration (e.g., first-order dependence when the aqueous and surface concentrations were low and the concentration of free surface sites was high and an apparent non-linear dependence as the aqueous and surface concentrations increased and the concentration of free surface sites was decreased). Whatever the mechanism of adsorption, all the kinetic models tested were able to describe the data within 0.1 RMSE.

## CONCLUSIONS

The results of this investigation have illustrated several salient aspects of U(VI) adsorption and transport in heterogeneous subsurface media. The rate of U(VI) adsorption exhibited a biphasic pattern, with rapid uptake occurring over the first few hours of the experiments followed by a period of slower adsorption. U(VI) non-linearly sorbed onto the three natural media, with a decrease in the extent of adsorption per unit aqueous concentration with increasing aqueous concentration. The observed adsorption nonlinearity is likely due to a decrease in the energetics of U(VI) adsorption to the' media with increased surface loading, and can be attributed to adsorption onto multiple site types in heterogeneous media, the most energetically-favored (i.e., strongest) sites being occupied first. The degree of adsorption was highly pH-dependent, with an increase in the extent of adsorption with the pH of the three media investigated. Similarities observed between the pH-dependent U(VI) adsorption on each media despite differences in bulk mineralogy

# REFERENCES


Allison, J. D., D. S. Brown and K. J. Novo-Gradac, 1991. MINTEQA2/PRODEFA2, A Geochemical Assessment Model for Environmental Systems: Version 3.0 User's Manual. EPA. Athens, GA.

Bruno, J., J. De Pablo, L. Duro and E. Figuerola, 1995. "Experimental study, and modeling of the U(VI)-$Fe(OH)_3$ surface precipitation/coprecipitation equilibria." *Geochim. Cosmochim. Acta.* 59(20): 4113-4123.

Casas, I., D. Casabona, L. Duro and J. Depablo, 1994. "The influence of hematite on the sorption of uranium(VI) onto granite filling fractures." *Chem. Geol.* 113: 319-326.

Chisholm-Brause, C., S. D. Conradson, C. T. Buscher, P. G. Eller and D. E. Morris, 1994. "Speciation of uranyl sorbed at multiple binding sites on montmorillonite." *Geochim. Cosmochim. Acta.* 58(17): 3625-3631.

Duff, M. C. and C. Amrhein, 1996. "Uranium(VI) adsorption on goethite and soil in carbonate solutions." *Soil Sci. Soc. Am. J.* 60(5): *1393-1400.*

Grenthe, I., 1992. Chemical Thermodynamics of Uranium. North-Holland. New York.

Hsi, C.-K. D. and D. Langmuir, 1985. "Adsorption of uranyl onto ferric oxyhydroxides: Application of the surface complexation site-binding model." *Geochim. Cosmochim. Acta. 49: 1931-1941.*

Jardine, P. M. 1991. "Modeling nonequilibrium reaction of inorganic solutes in soil columns." In: Rates of Soil Chemical Processes. Soil Science Society of America Special, Publication No. 27. Madison, WI. pp.255-279.

Kinniburgh, D. G., 1986. "General purpose adsorption isotherms." *Environ. Sci. Technol. 20: 895-904.*

Kohler, M., G. I?. Curtis, D. B. Kent and J. A. Davis, 1996. "Experimental investigation and modeling of uranium (VI) transport under variable chemical conditions." *Water Resour. Res.* 32(12): *3539-3551.*

Kohler, M., E. Wieland and J. 0. Leckie. 1992. "Metal-ligand-surface interactions during sorption of uranyl and neptunyl on oxides and silicates." In: Water-Rock Interaction. Kharaka and Maest (ed.). Balkema. Rotterdam. pp.51-54.

Ma, L. and H. M. Selim, 1997. "Evaluation of nonequilibrium models for predicting atrazine transport in soils." *Soil Sci. Soc. Am J* 61: 1299-1307

McKinley, J. P., J. M. Zachara, S. C. Smith and G. D. Turner, 1995. "The influence of uranyl hydrolysis and multiple site-binding reactions on adsorption of U(VI) to montmorillonite." *Clays Clay Miner.* 43(5): *586-598.*

Morris, D. E., C. J. Chisholm-Brause, M. E. Barr, S. D. Conradson and P. G. Eller, 1994. "Optical spectroscopic studies of the sorption of $UO_2^{2+}$ species on a reference smectite." *Geochim. Cosmochim. Acta.* 58(17): *3613-3623.*

Morrison, S. J., R. R. Spangler and V. S. Tripathi, 1995. "Adsorption of uranium(VI) on amorphous ferric oxyhydroxide at high concentrations of dissolved carbon(IV) and sulfur(VI)." Journal *of Contaminant Hydrology. 17: 333-346.*

Morse, J. W., P. M. Shanbhag, A. Saito and G. R. Choppin, 1984. "Interaction'of uranyl ions in carbonate media." *Chem. Geol. 42: 85-99.*

Parker, J. C. and M. T. van Genuchten, 1984. Determining Transport Parameters from Laboratory and Field Tracer Experiments. Virginia Agricultural Experiment Station. Bulletin 84-3.

Selim, H. M., M. C. Amacher and I. K. Iskandar, 1990. Modeling the Transport of Heavy Metals in Soils. U.S. Army Corps of Engineers. Monograph 90-Z.

Sims, R., T. A. Lawless, J. L. Alexander, D. G. Bennett and D. Read, 1996. "Uranium migration through intact sandstone: effect of pollutant concentration and the reversibility of uptake." *Journal of Contaminant Hydrology.* 21: 215-228.

Sposito, G., 1984. The Surface Chemistry of Soils. Oxford University Press. New York.

Szecsody, J. E., J. M. Zachara, A. Chilakapati, I?. M. Jardine and A. S. Ferrency, 1998. "Importance of flow and particle-scale heterogeneity on $Co^{II/III}EDTA$ reactive transport." *J. Hydrol. 209:* 112-136.

Ticknor, K. V., 1994. "Uranium sorption on geological materials." *Radiochim. Acta. 64: 229-236.*

Towle, S. N., J. R. Bargar, G. E. Brown and G. A. Parks, 1997. "Surface precipitation of Co(II)(aq) on $Al_2O_3$." *Journal of Colloid and Interface Science. 187:* 62-82.

Tripathi, V. J., 1983. Uranium(VI) Transport Modeling: Geochemical Data and Submodels. Ph.D. Dissertation. Stanford University.

Turner, G. D., J. M. Zachara, J. I? McKinley and S. C. Smith, 1996. "Surface-charge properties and $UO_2^{2+}$ adsorption of a subsurface smectite." *Geochim. Cosmochim. Acta.* 60(18): 3399-3414.

Voudrias, E. A. and J. L. Means, 1993. "Sorption of uranium by brine-saturated halite, mudstone and carbonate minerals." *Chemosphere.* 26(10):1753-1765.

Waite, T. D., J. A. Davis, T. E. Payne, G. A. Waychunas and N. Xu, 1994. "Uranium(VI) adsorption to ferrihydrite: Application of a surface complexation model." *Geochim. Cosmochim. Acta.* 58(24): *5465-5478.*

**Table 2 Adsorption isotherm parameters and statistics of model fit**

| Soil | $K_f$† | n t | $r^2$ |
|---|---|---|---|
| OR | 450 ± 30 | 0.67 ± 0.04 | 0.989 |
| SR | 230 ± 7 | 0.68 ± 0.02 | 0.995 |
| HF | 480 ± 10 | 0.56 ± 0.03 | 0.985 |

t $K_f$ is the adsorption capacity parameter and n is the adsorption intensity parameter. Results are shown as ±95% confidence intervals. Solid and aqueous phase U(VI) concentrations expressed in mg/kg and mg/L respectively.

Table 1 Physical, chemical, and mineralogical properties of the materials

| Material | Particle Size sand (%) | silt (%) | clay (%) | Mn (g/kg) | Fe (g/kg) | pH | organic matter (g/kg) | Mineralogy† |
|---|---|---|---|---|---|---|---|---|
| OR | 31 | 50 | 19 | 0.36 | 25.8 | 4.7 | 0.55 | $I_{30}IS_{25}K_{20}S_{10}V_{10}Q_5$ |
| SR | 69 | 7 | 24 | 0.06 | 25.7 | 4.1 | 0.12 | S>I>K>Q |
| HF | 98 | 2 | <1 | 4.0 | 25.3 | 6.8 | 0.13 | Q,M,HIV, P,Fe,Mn |

† Mineralogy for <2 μm fraction for OR and SR, bulk mineralogy for HF. I=illite, IS=interstratified 2:1, K=kaolinite, S=smectite, V=vermiculite, Q=quartz, M=mica, HIV=Hydroxy-interlayer vermiculite, P=plagioclase, Fe=Fe-oxides, Mn=Mn-oxides. Subscripts indicate percent by mass where known.

Wersin, P., M. F. Hochella Jr., I? Persson, G. Redden, J. 0. Leckie and D. W. Harris, 1994. "Interaction between aqueous uranium(VI) and sulfide minerals: Spectroscopic evidence for sorption and reduction." *Geochim. Cosmochim. Acta.* 58(13): *2829-2843.*

Zachara, J. M., P. L. Glassman, S. C. Smith and D. Taylor, 1995. "Oxidation and adsorption of Co(II)EDTA$^{2-}$ complexes in subsurface materials with iron and manganese oxide grain coatings." *Geochim. Cosmochim. Acta.* 59(21): 4449-4463.

Zachara, J. M. and G. l?. Streile, 1991. Use of Batch and Column Methodologies to Assess Utility Waste Leaching and Subsurface Chemical Attenuation. Electric Power Research Institute. EN-7313. Palo Alto, CA.

1 **Table 4 Modeling results of column transport experiments**

| Model† | RMSE | fitted parameter | estimated value‡ |
|---|---|---|---|
| Savannah River | | | |
| NLE | 0.568 | none | |
| NLE-FOK | 0.094 | $k_1$ | 2.8 ± 0.9 |
| | | $k_2$ | 0.002 ± 0.002 |
| FOK | 0.053 | $k_1$ | 15.6 f0.7 |
| | | $k_2$ | 0.019 ± 0.001 |
| FRK | 0.041 | $k_1$ | 22 ± 1 |
| | | $k_2$ | 0.020 ± 0.001 |
| | | m | 0.80 ± 0.03 |
| Oak Ridge | | | |
| NLE | 0.319 | none | |
| NLE-FOK | 0.047 | $k_1$ | 3000 ± 9000 |
| | | $k_2$ | 3 ± 9 |
| FOK | 0.070 | $k_1$ | 180 ± 8 |
| | | $k_2$ | 0.111 ± 0.005 |
| FRK | 0.036 | $k_1$ | 150 ± 20 |
| | | $k_2$ | 0.054 ± 0.005 |
| | | m | 0.66 ± 0.02 |
| Hanford | | | |
| NLE | 0.250 | none | |
| NLE-FOK | 0.048 | $k_1$ | 12 ± 1 |
| | | $k_2$ | 0.111 ± 0.005 |
| FOK | 0.079 | $k_1$ | 70 ± 20 |
| | | $k_2$ | 0.015 ± 0.004 |
| FRK | 0.042 | $k_1$ | 30 ± 3 |
| | | $k_2$ | 0.011 ± 0.001 |
| | | m | 0.62 ± 0.03 |

2 t NLE, nonlinear equilibrium; NLE-FOK, nonlinear equilibrium, first-
3 order kinetic; FOK, first-order kinetic; FRK, fractional order kinetic.

4 ‡ Estimated value ± the standard error. Units of $k_1$ and $k_2$ are $hr^{-1}$.

**Table 3 Adsorption as a function of pH†**

| Soil | $pH_{50}$-1 | $pH_{50}$-2 | $pH_{max}$ | Max. % ads. |
|---|---|---|---|---|
| OR | 4.4 | 8.2 | 6.5 | 98 |
| SR | 5.1 | 7.9 | 6.6 | 92 |
| HF | 4.7 | 7.6 | 6.1 | 90 |

† $pH_{50}$-1 and -2 are the pH where 50% of the U(VI) was adsorbed at lower and higher pH respectively, $pH_{max}$ is the pH where maximum adsorption occured, and Max % ads. is the maximum degree of adsorption observed.

1 ADSORPTION AND TRANSPORT U(VI) SUBSURFACE MEDIA, Fig. 1

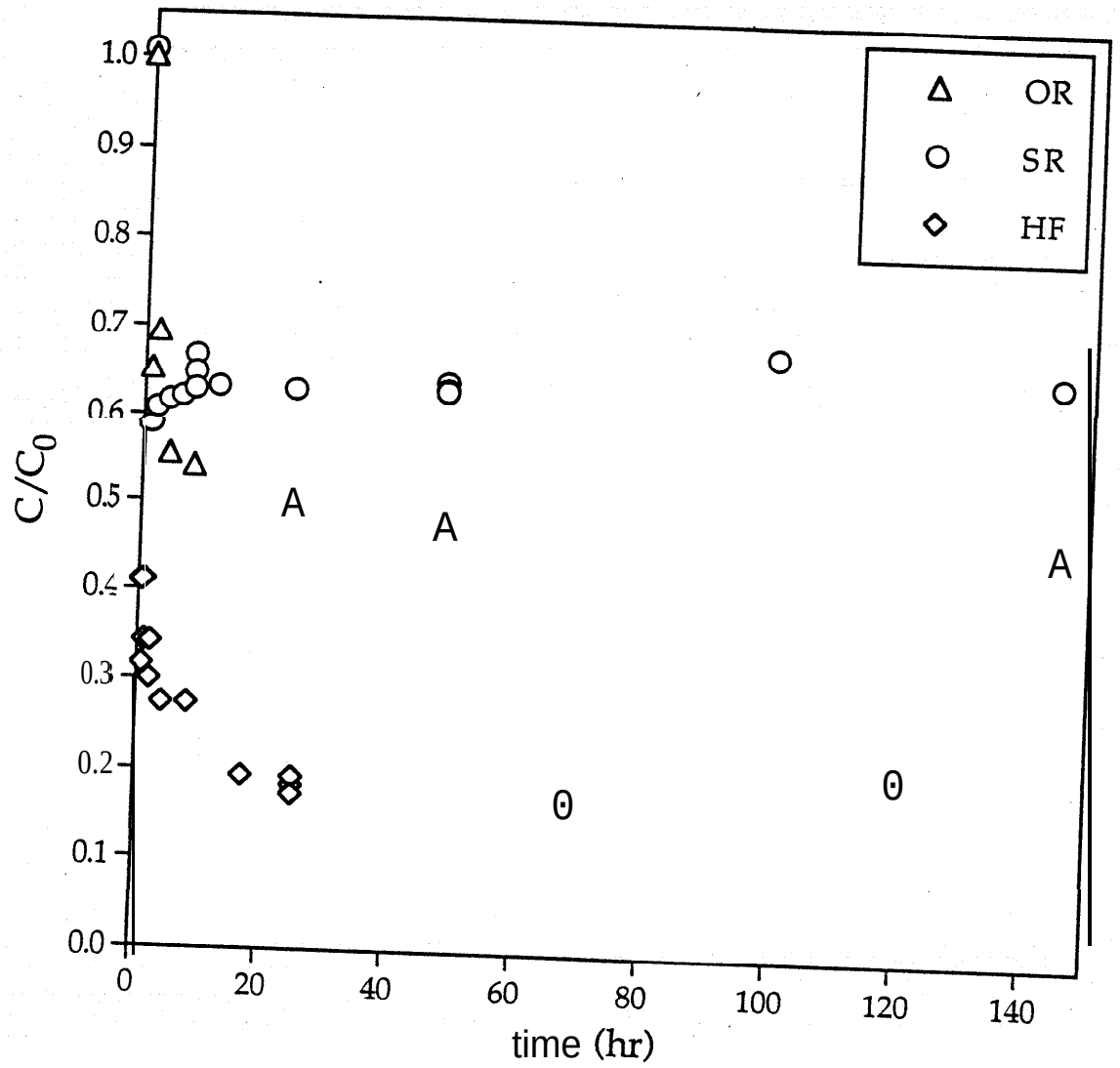

1 ADSORPTION AND TRANSPORT U(VI) SUBSURFACE MEDIA, Fig. 2

a)

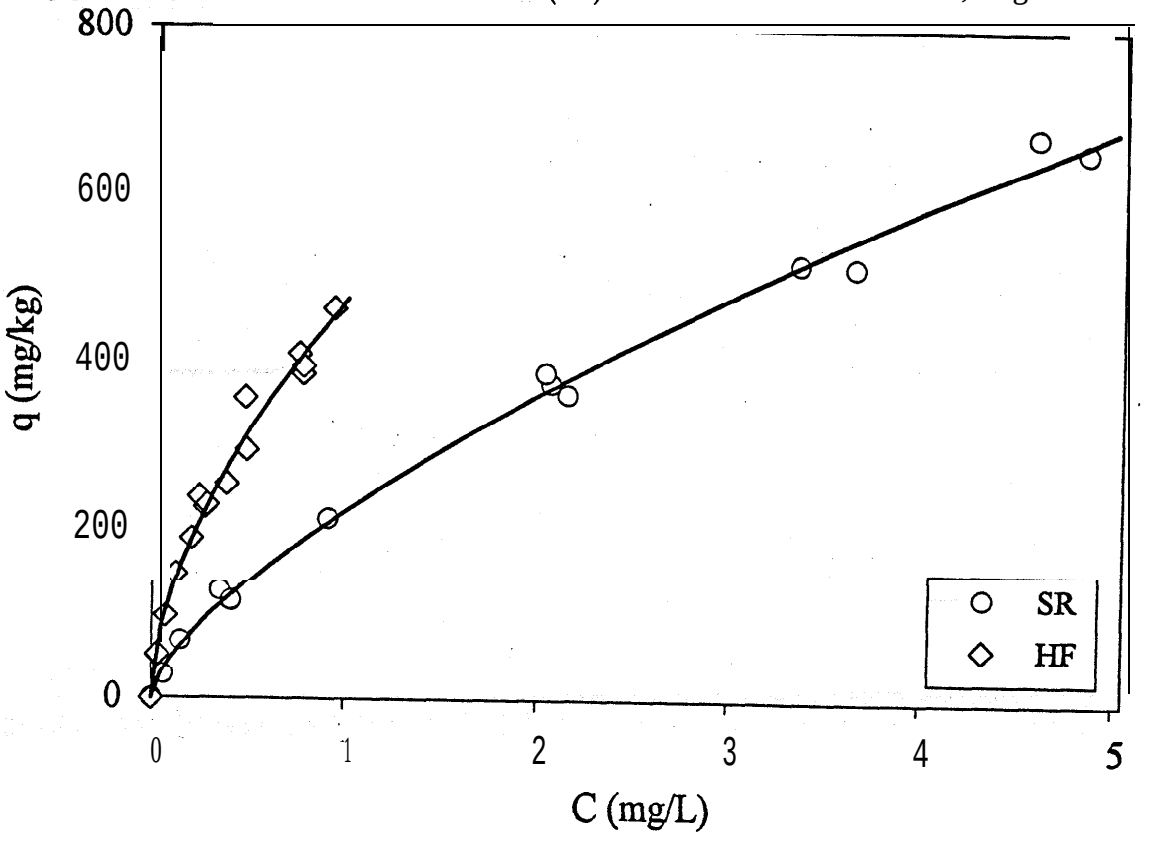


b)

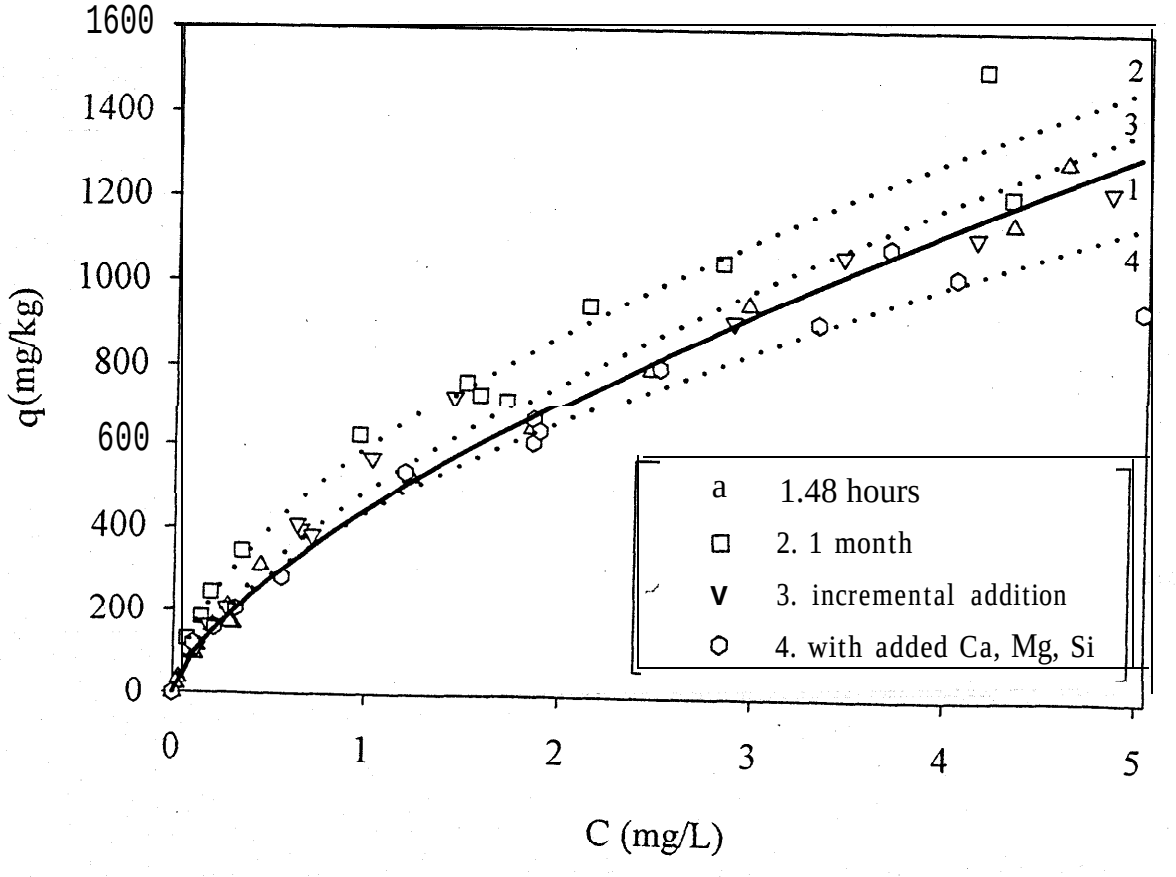

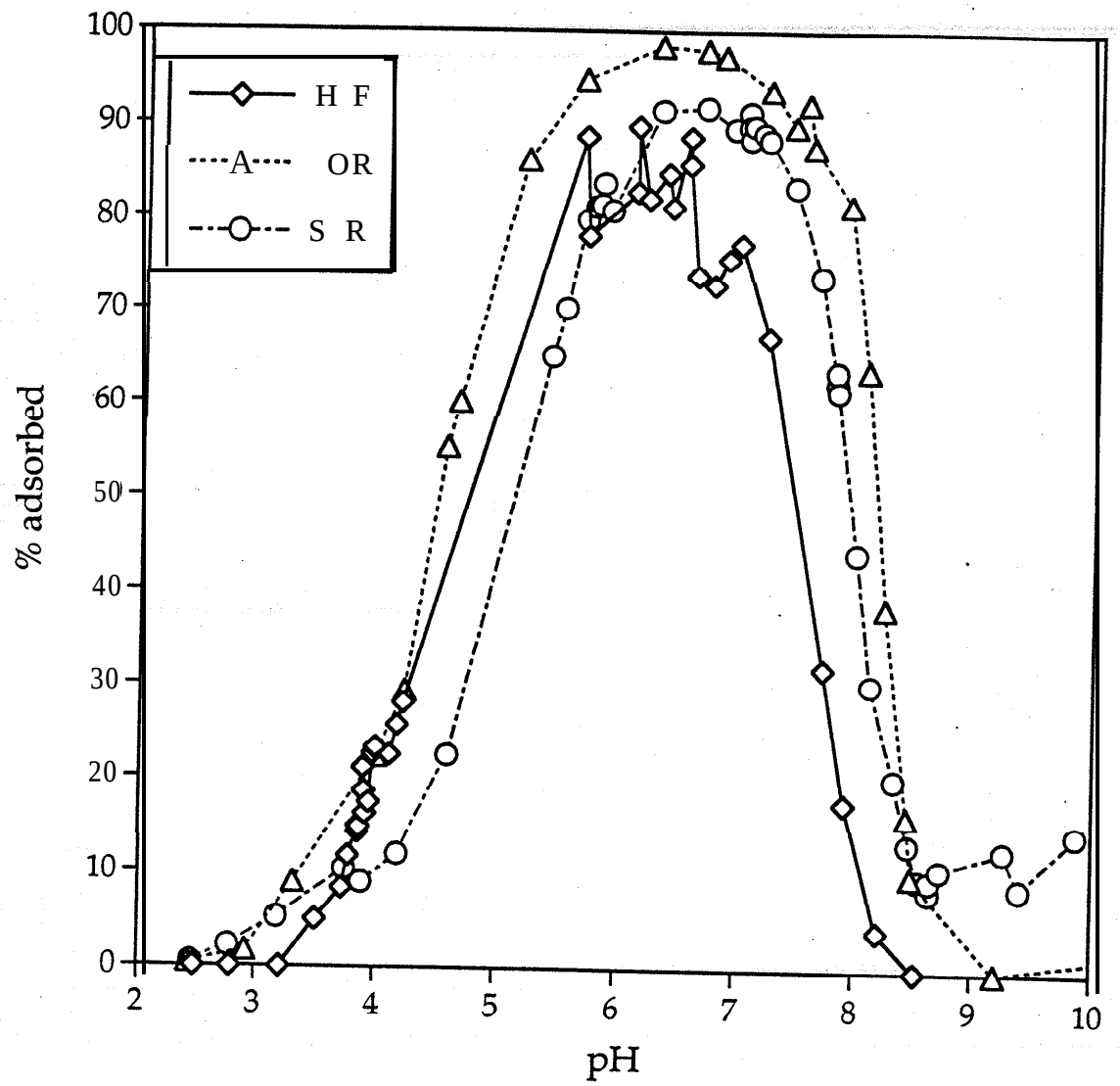
H F
A OR
S R
% adsorbed
pH
100
90
80
70
60
50
40
30
20
10
0
2
3
4
5
6
7
8
9
10

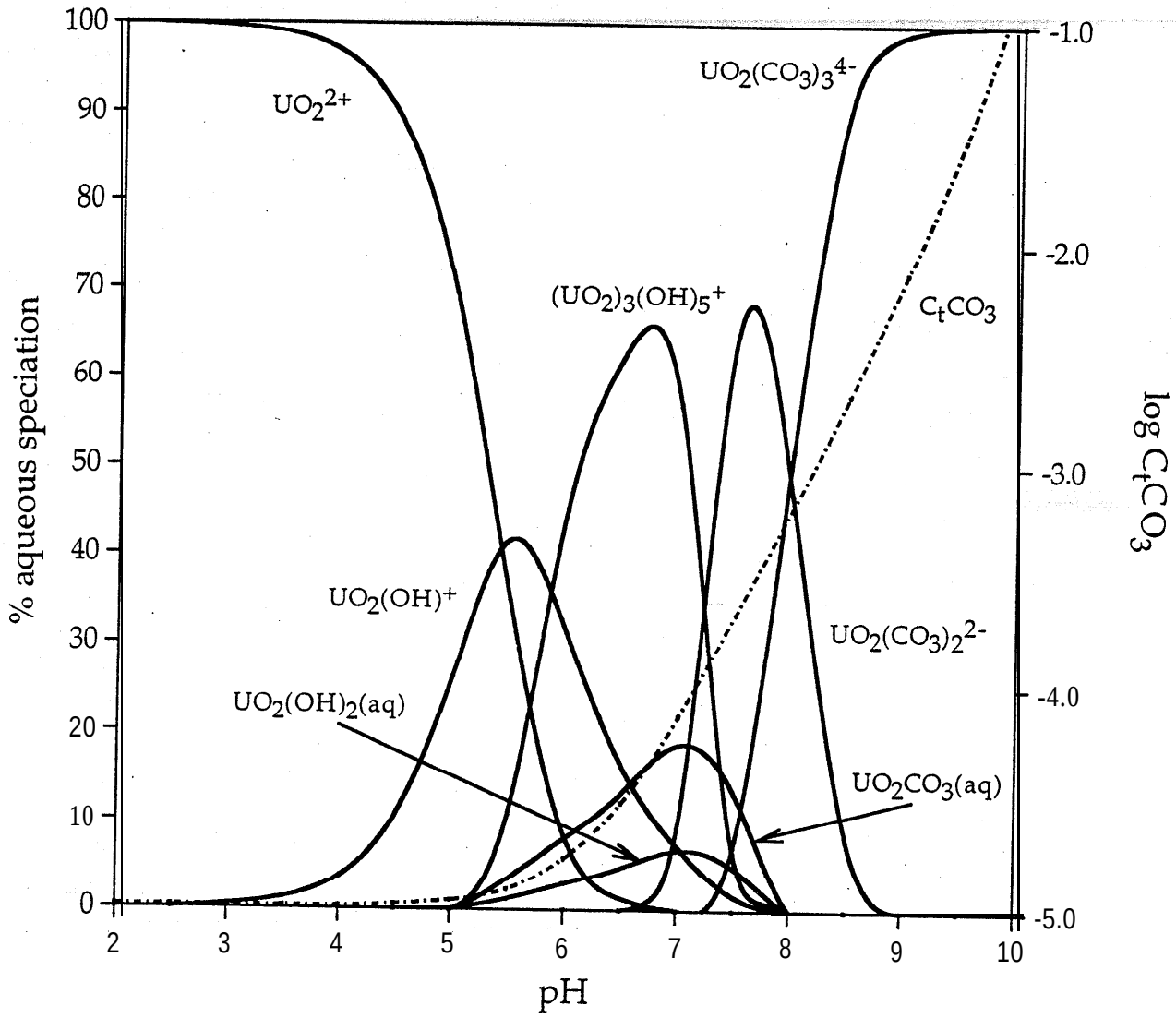
100
90
80
70
60
50
40
30
20
10
0
% aqueous speciation
-1.0
-2.0
-3.0
-4.0
-5.0
log $C_tCO_3$
2
3
4
5
6
7
8
9
10
pH
$UO_2^{2+}$
$UO_2(CO_3)_3^{4-}$
$(UO_2)_3(OH)_5^+$
$C_tCO_3$
$UO_2(OH)^+$
$UO_2(CO_3)_2^{2-}$
$UO_2(OH)_2(aq)$
$UO_2CO_3(aq)$

Fig. 1 Results of kinetic experiments: aqueous fraction as a function of time. Solid-solution ratio = 3.33 g/L in 0.01 N NaNO3 with log $P_{CO_2}$ = -3.5.. For OR and SR, $C_0$= 5 mg/L, for HF $C_0$ = 0.52 mg/L.

Fig. 2 Adsorbed versus aqueous concentration. Results determined from batch experiments with 3.33 g/L solid in 0.01 N $NaNO_3$ with log $P_{CO_2}$ = -3.5. Solid and dotted lines denote the fitted isotherm(s) .a. SR and HF. b. OR.

Fig. 3 Adsorption as a function of pH. Solid-solution ratio = 3.33 g/L in 0.1 N $NaNO_3$ with log $P_{CO_2}$ = -3.5. Total system U(VI) is 1 mg/L.

Fig. 4 Speciation of 1 mg/l U(VI) and log total dissolved carbonate concentration (broken line) as a function of pH. Calculations made with MINTEQA2 (Allison et al., 1991) using the standard thermodynamic database and data from Grenthe (1992). Calculations made for an open system with log $P_{CO_2}$ = -3.5 in 0.1 N $NaNO_3$.

Fig. 5 Observed and model calculated breakthrough curves for U(VI) in SR column. $C_0$ = 5.0 mg/L, pH = 4.1 in 0.01 N $NaNO_3$ with log $P_{CO_2}$ = -3.5. NLE, nonlinear equilibrium; NLE-FOK, nonlinear equilibrium, first-order kinetic; FOK, first-order kinetic (not shown for clarity); FRK, fractional order kinetic.

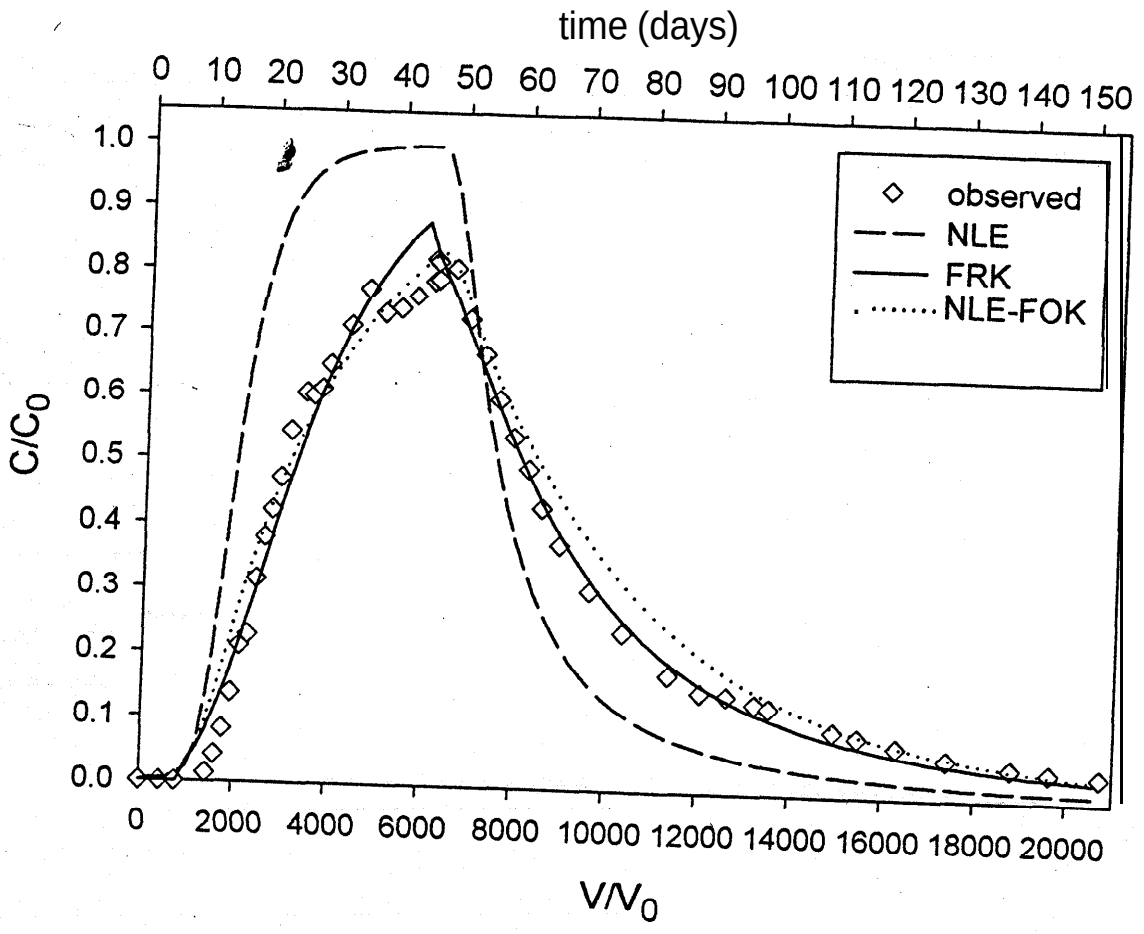
time (days)
0 10 20 30 40 50 60 70 80 90 100 110 120 130 140 150
1.0
0.9
0.8
0.7
0.6
0.5
0.4
0.3
0.2
0.1
0.0
C/C0
observed
NLE
FRK
NLE-FOK
0 2000 4000 6000 8000 10000 12000 14000 16000 18000 20000
V/V0

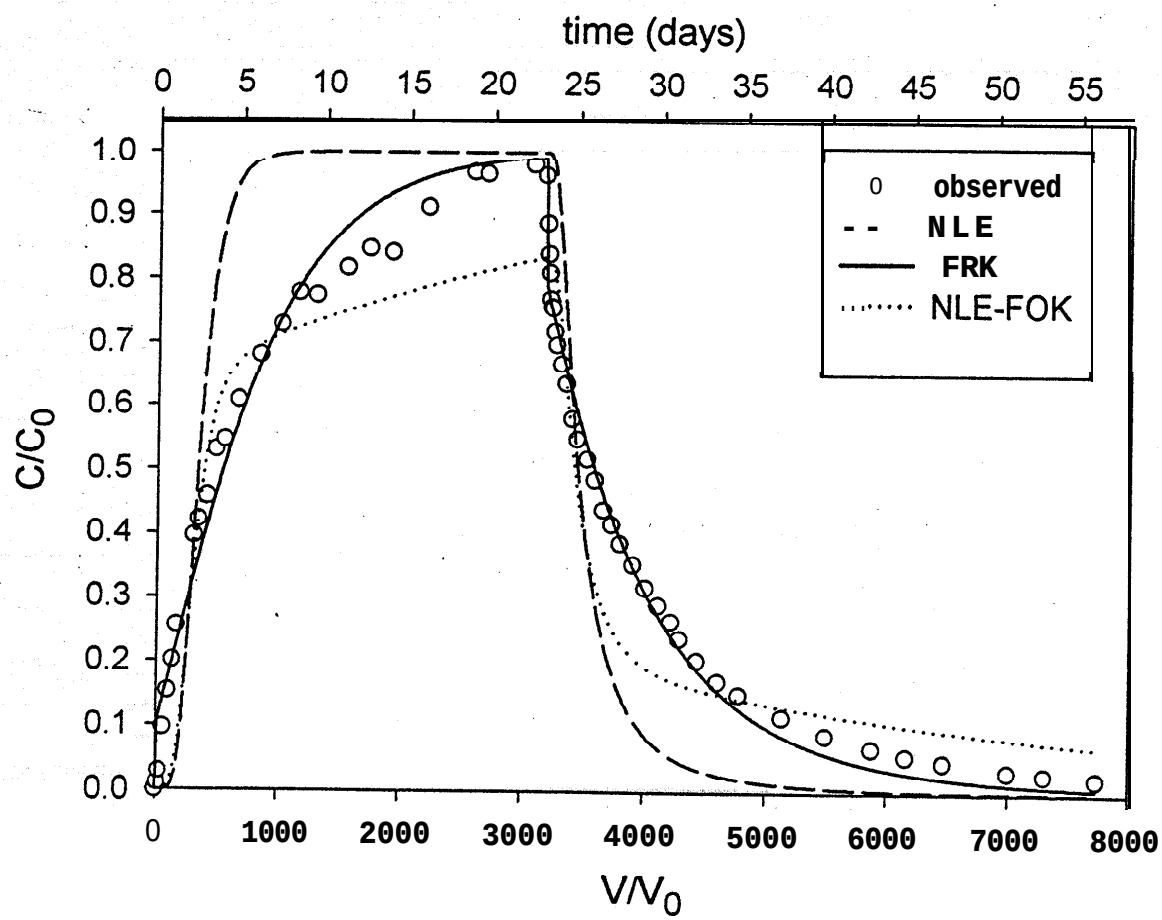
time (days)
0
5
10
15
20
25
30
35
40
45
50
55
1.0
0.9
0.8
0.7
0.6
0.5
0.4
0.3
0.2
0.1
0.0
C/C0
0
1000
2000
3000
4000
5000
6000
7000
8000
V/V0
observed
NLE
FRK
NLE-FOK